

Electrically Tunable and Reconfigurable Topological Edge State Lasers

Ruizhe Yao^{1†}, Hang Li^{2†}, Bowen Zheng², Sensong An², Jun Ding³, Chi-Sen Lee¹, Hualiang Zhang^{2*} and Wei Guo^{1*}

¹*Department of Physics and Applied Physics, University of Massachusetts Lowell, Lowell, Massachusetts, USA*

²*Department of Electrical & Computer Engineering, University of Massachusetts Lowell, Lowell, Massachusetts, USA*

³*School of Information and Science Technology, East China Normal University, Shanghai, China*

† These authors contributed equally to this work.

*hualiang_zhang@uml.edu, wei_guo@uml.edu

Abstract-We report an actively tunable topological edge mode laser in a one-dimensional Su-Schrieffer-Heeger (SSH) laser chain, where the SSH chain is realized in an electrically-injected Fabry-Perot (FP) laser array. A non-Hermitian SSH model is developed to investigate the SSH laser chain with tunable active topological defect. We theoretically demonstrate topological edge mode phase transition in the SSH laser chain. The phase transition manifested in the tight binding SSH laser chain is observed experimentally and agreed well with the theoretical predictions. Finally, by electronically tuning the gain and loss waveguides, a lossy topological mode is obtained, and trivial bulky mode lasing is experimentally observed. This work presents a versatile platform to investigate novel concepts, such as parity-time (PT) symmetry and topological mode, for main stream photonic applications.

1. Introduction

Topological insulators (TIs) introduce a new form of matter, which can support the flow of electrons on their surface but are insulator in their interior. Unlike surface states in normal insulators, the surface states in TIs are robust against perturbation and defects in the bulks[1-6]. Such tantalizing characteristics address the impurity issues in conventional bulk topology materials, and spark interests in the field of topological photonics [7-9]. Thus, it has drawn large interests in the investigation of topological phase transitions and edge-states in optical devices that are unaffected by local perturbations and fabrication defects [10-16]. However, most of such work has been focused on optical structures and devices with passive components. By incorporating active components in the photonic topological structures, it becomes possible to achieve lasing in these topological

edge-states. The resulting topological edge state lasers can exhibit low lasing threshold compared to the conventional bulk state lasers and are robust against any fabrication defects and local defects due to the temperature variations and any material degradations. The topological edge state lasers have been recently demonstrated in several systems[17-21], however, all of them are shown in optically pumped platforms which can largely limit the further exploration and applications of these unique topological lasers. In addition, it has been paid large attention in studying the interplay between non-Hermiticity and photonics topology devices. The optical non-Hermitian system is brought into attention by the notion of parity-time (PT) symmetry, where several new novel phenomena and optical devices have been proposed and demonstrated based on the PT symmetry in non-Hermitian systems [22-29]. In this context, topological lasers become an ideal

platform owing to the inherent non-Hermiticity in laser structures. In this report, we demonstrate lasing in topological edge state in one-dimensional Su-Schrieffer-Heeger (SSH) Fabry-Perot (FP) laser chain, which contains gain and loss waveguides and an active gain topological defect. The active topological defect is employed to enhance the density of state (DOS) of the topological edge state and ensure lasing at the lowest threshold compared to other bulk modes. Phase transition between the topological edge state and bulk state lasing is shown experimentally, and the PT symmetry phase transition in the topological mode laser is observed. Finally, by electrically tuning the gain and loss in the SSH laser chain, the topological defect mode becomes a lossy mode, and a trivial bulk mode lasing is observed at the lowest threshold.

2. Topological Laser Design

To achieve a photonics topological edge mode laser, we design a photonics topological insulator structure consisting of 7 pairs of coupled Fabry-Perot (FP) waveguide SSH dimers. Figure 1(a) shows the schematic of the dimer chain, where C_1 and C_2 represent the coupling efficiency between the gain (orange) and loss (blue) waveguides, and $C_1 > C_2$. The trivial and non-trivial topological states are achieved by strong and weak coupling in the dimers consisting of gain and loss, respectively. A topological defect in the chain is introduced by removing the loss waveguide in the middle dimer (4th pair). As a result, the designed active SSH chain consists of 13 coupled ridge waveguide lasers with the width of 3 μm . The laser active region is composed of 7-layer InAs quantum-dots (QDs) sandwiched between $\text{Al}_{0.4}\text{Ga}_{0.6}\text{As}$ cladding layers. Figure 1(b) shows the heterostructures of the InAs QD lasers grown by molecular beam epitaxy (MBE) system. In the laser array, the top p+-GaAs contact layer and p- $\text{Al}_{0.4}\text{Ga}_{0.6}\text{As}$ cladding layer are etched for electrical isolation between each waveguide. The coupling strengths, C_1 and C_2 , in the dimers are controlled by the width of the isolation trenches, 1 μm and 2 μm , respectively. All the gain and loss waveguides are interconnected allowing simultaneous and fully electronic control of all the gain and loss waveguides.

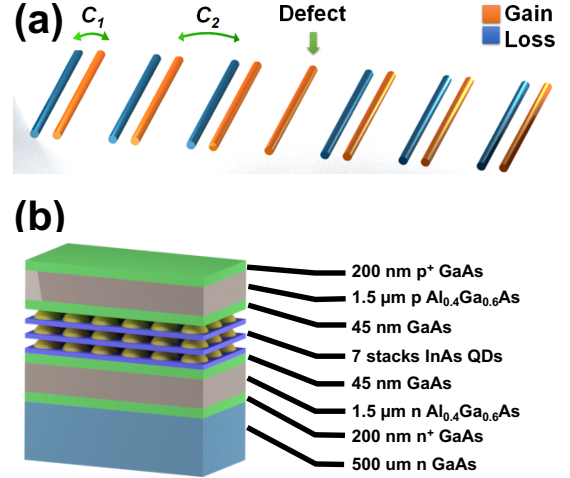


FIG. 1: (a) Schematic of the dimer chain, where C_1 and C_2 represent the coupling efficiency between the gain (orange) and loss (blue) waveguides, and $C_1 > C_2$. (b) heterostructures of the InAs QD lasers grown by molecular beam epitaxy.

3. Non-Hermitian SSH Model

A one-dimensional SSH model is first employed to investigate the passive Hermitian dimer chain without gain and loss [30]. The SSH model studies two sites per unit cell with different coupling efficiency C_1 and C_2 . It is well understood that, in SSH mode, the edge states depend on the configuration of the unit cell. The edge state exists only when the smaller coupling, C_2 , is located at the edges [30, 31]. In contrast, there is no edge state if the chain is terminated by a dimer with larger coupling efficiency, C_1 . These two different scenarios can be identified by the winding number in Brillouin zone (BZ) SSH model [32]:

$$W_h = \frac{1}{2\pi} \int_{\text{BZ}} dk \frac{\partial \psi(k)}{\partial k} \quad (1)$$

where k is the Bloch wavenumber within the first BZ, and the winding number is corresponding to the Zak phase (ψ_{ZAK}) divided by π [33]. It has been shown that, when $W_h=1$, the system exhibits trivial topological phase without edge states, in contrast, if $W_h=0$, the system transits into non-trivial topological phase with two edge states presented[34]. As a result, in the explored topological configuration, the defect waveguide,

4th pair dimer with gain waveguide only, is located at an interface between two structures that have different topological invariants, $W_h = 0, 1$. Thus, there must be a topological interface state residing at zero energy at the defect waveguide. Szameit *et. al.* has already investigated such topological waveguide configuration containing passive components and shown the topological edge mode appearing in the center defect while preserving the PT symmetry [35]. In this work, we employ the dimer chain containing gain and loss and an active, gain, defect to achieve topological laser. It has been argued that, if an active defect is introduced, the topological edge state can be enhanced by supplementing the topological protection with non-Hermitian symmetries [36]. In this context, a non-Hermitian SSH model is employed to explore the density of state (DOS) of the topologically zero energy mode. As shown in Figure 2, the DOS of the zero-energy mode is largely enhanced by including an active defect compared to the passive defect case. It is worth noting that the DOS enhancement can be obtained not only with the active defect but also with an absorptive lossy defect due to the symmetry of the Hamiltonian [36].

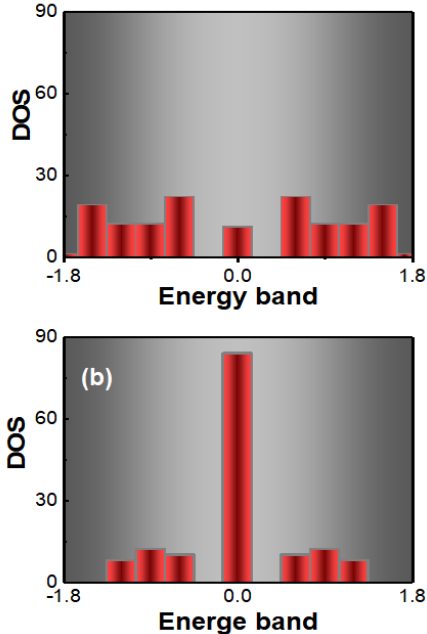


FIG. 2: Density of state (DOS) of the topologically zero energy mode without (a) and with (b) active defect, the DOS of the zero-energy mode is largely enhanced by including an active defect compared to the passive defect case.

In addition, it is also of large interests to investigate the PT symmetry in the proposed gain/loss non-Hermitian SSH system. As discussed by Szameit *et. al.* [35], the PT symmetry is always preserved in the passive dimer chain with a neutral defect [35]. In our case, the active gain defect explicitly breaks the PT symmetry, preventing the Hamiltonian from commuting with the PT operators, $[PT, H] \neq 0$. This topologically induced property can further enhance the mode competition. The topological defect state is predominately located in the gain defect waveguides and is isolated from loss waveguides affecting all other modes in the system, which can reduce the lasing thresholds of the topological mode, even in presence of structural disorder. Figure 3 shows the eigenvalue diagrams and corresponding optical field distributions at different gain, g , values, where a dimensionless variable $v=g/C_l$ is defined in this work. It is found that the edge mode exhibits complex eigenvalues, with gain, as long as the system gain is non-zero and all the optical field are predominately located in the defect gain waveguide in the SSH system and symmetrically distributed around the defect waveguide. Finally, the dynamics of the proposed SSH laser is theoretically investigated. Three distinguished phases are observed in Figure 3(a)-(d). In phase I, only the edge mode exhibits complex eigenvalue with gain, and the SSH laser array is lasing at single topological mode. The corresponding dispersion relation of the lasing edge mode and optical field distribution are plotted in Figure 3(a). By increasing the gain, in phase II, one trivial bulk mode is transited into a phase with complex eigenvalue and will start to lase alongside with edge mode. Figure 3(b) shows the dispersion relation of the lasing edge mode with complex eigenvalue and the corresponding optical field distribution of the lasing bulk mode. Finally, with further increase of the gain, other bulk modes will show complex eigenvalues and the gains of these bulk modes will be comparable with the edge mode. Therefore, the edge mode becomes less dominant and this in turn results in a more uniform mode intensity profile across the SSH chain under investigation. The dispersion relation and optical field distribution of the second bulk mode under this case are shown in Figure 3(c).

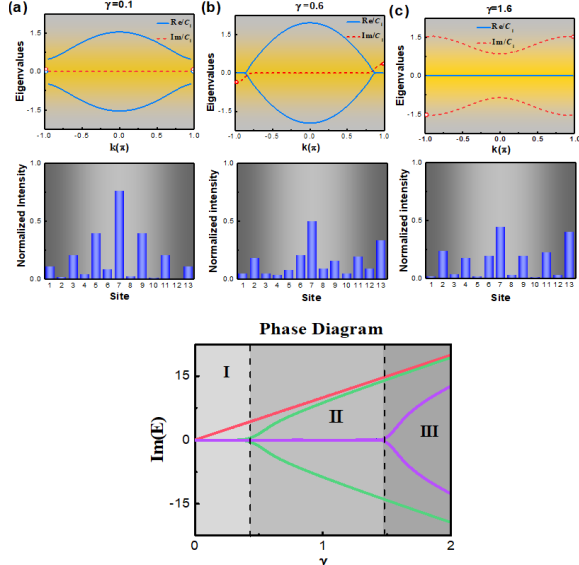


FIG 3: Eigenvalue diagram of SSH chain of in Phase I (a), II (b) and III (c); the insets below shows the corresponding optical intensity distributions; (d) Phase diagram of the complex SSH chain.

Finally, Figure 4(a) plots the band diagram of non-Hermitian topological system. It is clearly seen that the topological band gap doesn't close in the non-Hermitian topological system and no topological phase transition is observed, this indicates that the system retains its topological properties with the presence of gain. In addition, in Figure 4(b), the complex frequency, shown in blue dots, possesses a single non-degenerated topological mode with gain. By further increasing the system gain level, shown in red dots, the gain of topological mode will be further increased, while other bulk modes will also be transited into lasing modes by having complex eigenfrequencies. This process explicitly explains the mode selection between non-Hermitian topological mode and trivial bulk modes.

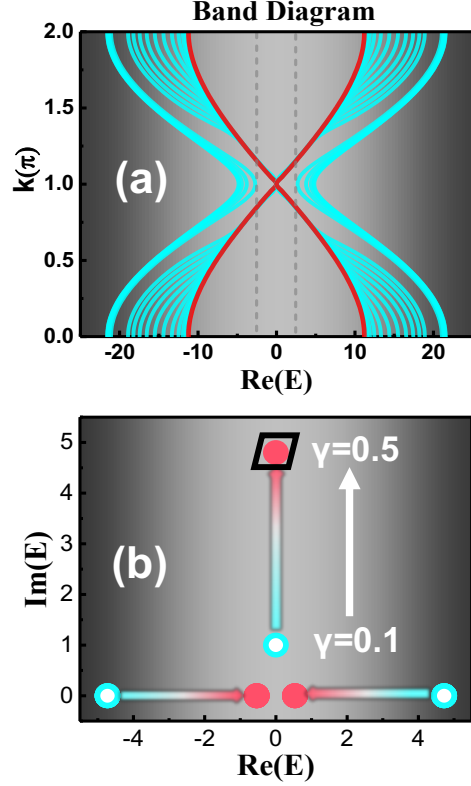


FIG 4: (a) Band diagram of non-Hermitian topological system. It is clearly seen that the topological band gap doesn't close in the non-Hermitian topological system and no topological phase transition is observed, this indicates that the system retains its topological properties with the presence of gain. (b) complex frequency, shown in blue dots, possesses a single non-degenerated topological mode with gain. By further increasing the system gain level, shown in red dots, the gain of topological mode will be further increased, while other bulk modes will also be transited into lasing modes by having complex eigenfrequencies.

4. Results

In the experimental demonstration, the gain/loss SSH chain is achieved by electrically biasing the gain and loss waveguides at different levels. The bias current for the loss waveguides is maintained at 0 mA, which corresponds to a loss of $\sim 35 \text{ cm}^{-1}$ in the loss waveguide, and the gain waveguide bias current is varied from 0 to 1000 mA to electrically tune the gain in the gain waveguides. Figure 5 shows the light-current (L-I) characteristic of the SSH coupled waveguide

laser array. It is observed that the lasing threshold current is ~ 600 mA. The inset shows the electroluminescence (EL) spectrum of the laser chain. The lasing wavelength at $1.32 \mu\text{m}$ is obtained.

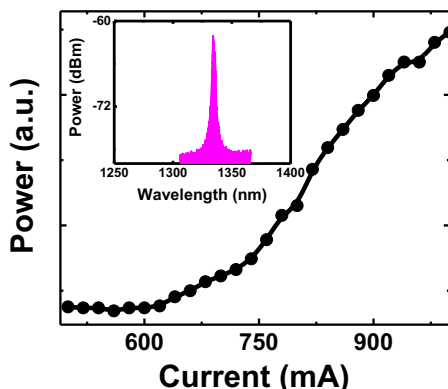


FIG 5: Light-current (L-I) characteristic of the SSH coupled waveguide laser array. It is observed that the lasing threshold current is ~ 600 mA. Inset: Electroluminescence (EL) spectrum of the laser chain.

The near-field pattern of the SSH laser chain is measured to understand the dynamics of the topological mode lasing and mode selections. Shown in Figure 6, the near-field patterns from the laser array are measured at various gain bias currents. When the gain bias current is small, 630 mA, the SSH laser array only lases at the topological mode in the center defect and the mode profile exhibits intensity maximum at the center defect and symmetrically distributed around the defect waveguide, site 7. When the bias current is increased to 700 mA, the first trivial bulk mode obtains enough gain and transit to lasing mode, while the topological mode is still dominating in the near-field profile. The SSH laser system evolves to phase II. With further increment of the bias current to 770 mA, more trivial bulk modes start to obtain enough gain and eventually transform to lasing modes, which leads to a more uniform near-field profile across the laser chain, and the system is transitioned into phase III. The experimental observation shows clear phase transitions of the topological mode laser and agrees well with the theoretical predications, Figure 3(d).

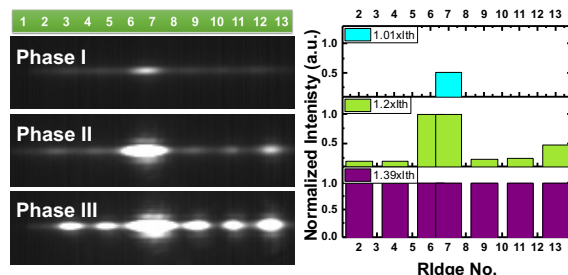


FIG 6: Near-field patterns measured at various gain bias currents. When the gain bias current is small, 630 mA (a), the SSH laser array only lases at the topological mode in the center defect and the mode profile exhibits intensity maximum at the center defect and symmetrically distributed around the defect waveguide, site 7. When the bias current is increased to 700 mA (b), the first trivial bulk mode obtains enough gain and transit to lasing mode, while the topological mode is still dominating in the near-field profile. The SSH laser system evolves to phase II. With further increment of the bias current to 770 mA (c), more trivial bulk modes start to obtain enough gain and eventually transform to lasing modes, which leads to a more uniform near-field profile across the laser chain, and the system is transitioned into phase III.

Finally, we also investigate a topological configuration with a lossy topological defect in the SSH chain. In the experiment, owing to the versatility of the electrically injected system, the lossy topological defect is simply achieved by interchanging the gain and loss waveguide bias currents. As compared in Figure 7(a), the system (after the electrically switched reconfiguration) still features the same topological configuration as in the case discussed before, but now with a lossy defect at the topological interface. The corresponding dispersion relations shows that the topological mode exhibits net loss and lasing is prohibited. As a result, the SSH laser chain will first lase at one of the trivial bulk modes with the highest gain. This is experimentally demonstrated as well by measuring the near-field pattern in the lossy topological defect SSH laser. Shown in Figure 7(b), instead of the single topological mode lasing, the system now first lases at a bulk mode which agrees well with the theoretical

prediction, where the near-field pattern of the original gain topological laser is shown as well for comparisons.

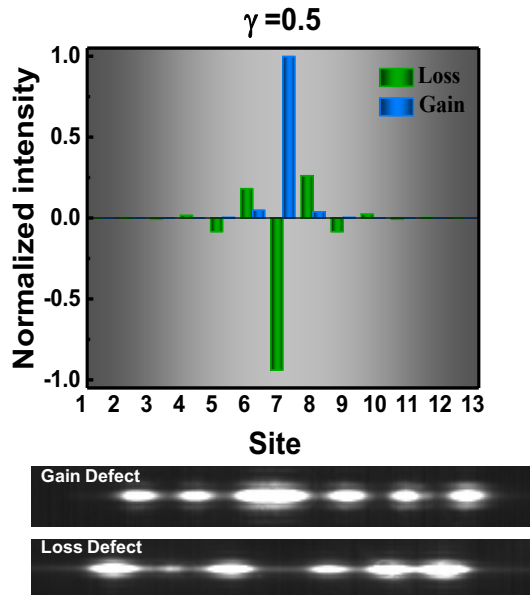


FIG 7: Comparison of topological states with loss (green) and gain (blue) defect (a) and near-field characteristics (b)

5. Conclusion

In summary, we have demonstrated an electrically-injected topological edge mode laser in a SSH chain with an active gain topological defect. The explored laser system is described by non-Hermitian SSH model. Phase transitions between topological and bulk mode lasing are observed. The experimental results are in good agreement with theoretical predictions. This work demonstrates a versatile electrically tunable platform and provides new perspectives in understanding some of the fundamentals in non-Hermitian topological systems.

6. Acknowledgements

R.Y. and W.G. acknowledge funding support from Massachusetts Clean Energy program. H.L., B.Z., S.A., and H.Z. gratefully thank funding support provided by DARPA under the Extreme Optics and Imaging (EXTREME) Program managed by Dr. Predrag Milojkovic. The authors also acknowledge fabrication

facility support by the Harvard University Center for Nanoscale Systems funded by the National Science Foundation under award 0335765.

7. Author contributions

W.G. and H.Z. conceived the ideas. R.Y. and C.S.L. contributed to the growth and fabrication the devices. R.Y. and H.L. performed device characterizations. H.L. modeled the device. H.L., R.Y., B.Z., S.A., J.D., H.Z., and W.G. analyzed the experimental data. W.G. and H.Z. supervised and coordinated the project. H.L., R.Y., H.Z., and W.G. wrote the manuscript. All authors contributed to technical discussions regarding this work.

8. Competing financial interests

The authors declare no competing financial interests.

9. References

- [1] X.-L. Qi, T.L. Hughes, S.-C. Zhang, Topological field theory of time-reversal invariant insulators, *Physical Review B*, 78 (2008) 195424.
- [2] L. Fu, C.L. Kane, Topological insulators with inversion symmetry, *Physical Review B*, 76 (2007) 045302.
- [3] M. König, S. Wiedmann, C. Brüne, A. Roth, H. Buhmann, L.W. Molenkamp, X.-L. Qi, S.-C. Zhang, Quantum Spin Hall Insulator State in HgTe Quantum Wells, *Science*, 318 (2007) 766.
- [4] D. Hsieh, D. Qian, L. Wray, Y. Xia, Y.S. Hor, R.J. Cava, M.Z. Hasan, A topological Dirac insulator in a quantum spin Hall phase, *Nature*, 452 (2008) 970.
- [5] D. Hsieh, Y. Xia, D. Qian, L. Wray, F. Meier, J.H. Dil, J. Osterwalder, L. Patthey, A.V. Fedorov, H. Lin, A. Bansil, D. Grauer, Y.S. Hor, R.J. Cava, M.Z. Hasan,

Observation of Time-Reversal-Protected Single-Dirac-Cone Topological-Insulator States in Bi_2Te_3 and Sb_2Te_3 , Physical Review Letters, 103 (2009) 146401.

[6] M.Z. Hasan, C.L. Kane, Colloquium: Topological insulators, Reviews of Modern Physics, 82 (2010) 3045-3067.

[7] X.-L. Qi, S.-C. Zhang, The quantum spin Hall effect and topological insulators, Physics Today, 63 (2009) 33-38.

[8] X.-L. Qi, S.-C. Zhang, Topological insulators and superconductors, Reviews of Modern Physics, 83 (2011) 1057-1110.

[9] L. Fu, C.L. Kane, Superconducting Proximity Effect and Majorana Fermions at the Surface of a Topological Insulator, Physical Review Letters, 100 (2008) 096407.

[10] M.C. Rechtsman, J.M. Zeuner, Y. Plotnik, Y. Lumer, D. Podolsky, F. Dreisow, S. Nolte, M. Segev, A. Szameit, Photonic Floquet topological insulators, Nature, 496 (2013) 196.

[11] R.O. Umucalı, I. Carusotto, Artificial gauge field for photons in coupled cavity arrays, Physical Review A, 84 (2011) 043804.

[12] M. Hafezi, E.A. Demler, M.D. Lukin, J.M. Taylor, Robust optical delay lines with topological protection, Nature Physics, 7 (2011) 907.

[13] K. Fang, Z. Yu, S. Fan, Realizing effective magnetic field for photons by controlling the phase of dynamic modulation, Nature Photonics, 6 (2012) 782.

[14] M. Hafezi, S. Mittal, J. Fan, A. Migdall, J.M. Taylor, Imaging topological edge states in silicon photonics, Nature Photonics, 7 (2013) 1001.

[15] X. Cheng, C. Jouvaud, X. Ni, S.H. Mousavi, A.Z. Genack, A.B. Khanikaev, Robust reconfigurable electromagnetic pathways within a photonic topological insulator, Nature Materials, 15 (2016) 542.

[16] L. Lu, J.D. Joannopoulos, M. Soljačić, Topological photonics, Nature Photonics, 8 (2014) 821.

[17] M.A. Bandres, S. Wittek, G. Harari, M. Parto, J. Ren, M. Segev, D.N. Christodoulides, M. Khajavikhan, Topological insulator laser: Experiments, Science, DOI 10.1126/science.aar4005(2018).

[18] M. Parto, S. Wittek, H. Hodaei, G. Harari, M.A. Bandres, J. Ren, M.C. Rechtsman, M. Segev, D.N. Christodoulides, M. Khajavikhan, Complex edge-state phase transitions in 1D topological laser arrays, arXiv preprint arXiv:1709.00523, DOI (2017).

[19] H. Zhao, P. Miao, M.H. Teimourpour, S. Malzard, R. El-Ganainy, H. Schomerus, L. Feng, Topological hybrid silicon microlasers, Nature communications, 9 (2018) 981.

[20] P. St-Jean, V. Goblot, E. Galopin, A. Lemaître, T. Ozawa, L. Le Gratiet, I. Sagnes, J. Bloch, A. Amo, Lasing in topological edge states of a one-dimensional lattice, Nature Photonics, 11 (2017) 651-656.

[21] M. Parto, S. Wittek, H. Hodaei, G. Harari, M.A. Bandres, J. Ren, M.C. Rechtsman, M. Segev, D.N. Christodoulides, M. Khajavikhan, Edge-

Mode Lasing in 1D Topological Active Arrays, *Physical Review Letters*, 120 (2018) 113901.

[22] C.E. Rüter, K.G. Makris, R. El-Ganainy, D.N. Christodoulides, M. Segev, D. Kip, Observation of parity–time symmetry in optics, *Nature physics*, 6 (2010) 192.

[23] A. Guo, G. Salamo, D. Duchesne, R. Morandotti, M. Volatier-Ravat, V. Aimez, G. Siviloglou, D. Christodoulides, Observation of P T-symmetry breaking in complex optical potentials, *Physical Review Letters*, 103 (2009) 093902.

[24] R. El-Ganainy, K. Makris, D. Christodoulides, Z.H. Musslimani, Theory of coupled optical PT-symmetric structures, *Optics letters*, 32 (2007) 2632-2634.

[25] L. Feng, M. Ayache, J. Huang, Y.-L. Xu, M.-H. Lu, Y.-F. Chen, Y. Fainman, A. Scherer, Nonreciprocal light propagation in a silicon photonic circuit, *Science*, 333 (2011) 729-733.

[26] B. Peng, Ş.K. Özdemir, F. Lei, F. Monifi, M. Gianfreda, G.L. Long, S. Fan, F. Nori, C.M. Bender, L. Yang, Parity–time-symmetric whispering-gallery microcavities, *Nature Physics*, 10 (2014) 394.

[27] L. Feng, Z.J. Wong, R.-M. Ma, Y. Wang, X. Zhang, Single-mode laser by parity-time symmetry breaking, *Science*, 346 (2014) 972-975.

[28] Y. Chong, L. Ge, A.D. Stone, P t-symmetry breaking and laser-absorber modes in optical scattering systems, *Physical Review Letters*, 106 (2011) 093902.

[29] H. Hodaei, M.-A. Miri, M. Heinrich, D.N. Christodoulides, M. Khajavikhan, Parity-time–symmetric microring lasers, *Science*, 346 (2014) 975-978.

[30] W.P. Su, J. Schrieffer, A.J. Heeger, Solitons in polyacetylene, *Physical Review Letters*, 42 (1979) 1698.

[31] N. Malkova, I. Hromada, X. Wang, G. Bryant, Z. Chen, Observation of optical Shockley-like surface states in photonic superlattices, *Optics letters*, 34 (2009) 1633-1635.

[32] P. Delplace, D. Ullmo, G. Montambaux, Zak phase and the existence of edge states in graphene, *Physical Review B*, 84 (2011) 195452.

[33] J. Zak, Berry’s phase for energy bands in solids, *Physical review letters*, 62 (1989) 2747.

[34] C.M. Bender, M. DeKieviet, S.P. Klevansky, PT quantum mechanics, *Philos Trans A Math Phys Eng Sci*, 371 (2013) 20120523.

[35] S. Weimann, M. Kremer, Y. Plotnik, Y. Lumer, S. Nolte, K.G. Makris, M. Segev, M.C. Rechtsman, A. Szameit, Topologically protected bound states in photonic parity–time-symmetric crystals, *Nature Materials*, 16 (2016) 433.

[36] C. Poli, M. Bellec, U. Kuhl, F. Mortessagne, H. Schomerus, Selective enhancement of topologically induced interface states in a dielectric resonator chain, *Nature communications*, 6 (2015) 6710.